

Supporting Information

Gigoux et al. 10.1073/pnas.0911573106

SI Text

Generation of ICOS-YF Mice. We designed a targeting construct such that the exon 3 of the wild-type *Icos* gene will be replaced by an engineered exon 3 and a neomycin-resistance (Neo) cassette flanked by two loxP elements (Fig. S1A). The engineered exon 3 contained an adenine-to-thymidine change that results in a tyrosine-to-phenylalanine mutation at amino acid 181 of the cytoplasmic tail of ICOS. Using an *EcoRI* site created by the mutation, we identified ES clones (R1, 129 background) that have integrated the mutant allele by Southern blot analysis (Fig. S1B) and subsequently verified the intended mutation by sequencing the PCR products generated from the gene-targeted ES cells (Fig. S1C). We injected the ES cells into the blastocysts (C57BL/6 background), and resulting chimeric mice were backcrossed with C57BL/6 mice. Mice with germline transmitted *Icos* (*Y181F*)-*Neo* allele were bred with CMV-Cre transgenic mice (1) to achieve in vivo deletion of Neo cassette (Fig. S1D). We also verified that the mRNA transcribed from *Icos*^{*Y181F*} locus has the same structure as the WT *Icos* mRNA, except for the point mutation by sequencing PCR-amplified cDNA fragments encompassing exon 2 to exon 5.

Antibodies and Cytokines. For flow cytometry or T-cell stimulation, the following antibodies were used: Armenian hamster IgG, antibodies against ICOS (mAb C398.4A for stimulation and 5F9 for staining), CD3 (145.2C11), CD4, CD8, CD16/32 (Fc block), Fas, IgD, PD-1 (all purchased from eBioscience), and GL7 (BD). Goat anti-Armenian hamster IgG (Jackson ImmunoResearch) or avidin (Calbiochem) were used to cross-link primary antibodies. Biotinylated anti-CXCR5 (BD) was used with streptavidin-APC or -PE (eBioscience). For immunoblots, goat anti-mouse ICOS (sc 5748; Santa Cruz) and rabbit anti-PI3K p85 α (Upstate Biotechnology) and antibodies against phospho-specific or total Akt, p44/42 MAPK, JNK, p38 (Cell Signaling Technology) were

used with HRP-conjugated anti-goat (sc2020; Santa Cruz) or anti-rabbit (Bio-Rad Laboratories) secondary antibodies. Recombinant IL-2 was purchased from R&D Systems and IL-6 from eBioscience.

Ca²⁺ Flux. CD4⁺ T blasts were loaded with Indo-1 (Invitrogen) at 5×10^6 cells/mL in HBSS buffer supplemented with 0.1% BSA, 1 mM CaCl₂, and 1 μ M MgCl₂. Cells were incubated for 1 min at RT with biotinylated antibodies: 0.1 μ g/mL anti-CD3 plus 1 μ g/mL anti-ICOS (1 μ g/mL) or control hamster IgG. After recording baseline for 30 s, avidin (14 μ g/mL) was added, and the mobilization of intracellular Ca²⁺ was monitored by measuring FL4/FL5 on LSR FACS machine (BD). Equal loading of Indo-1 was confirmed by releasing intracellular Ca²⁺ by ionomycin (1 μ g/mL; Sigma-Aldrich).

Immunization of Mice. NP₁₆-CGG (1 mg/mL in PBS; Biosearch Technologies) was mixed with an equal volume of Imject Alum (Thermo Scientific) for 30 min at room temperature. Mice were injected i.p. with 100 μ g (primary) or 50 μ g (secondary) of alum-precipitated NP₁₆-CGG.

ELISA. Various isotypes of mouse Ig were detected using mouse Ig isotyping kit (SouthernBiotech). Fecal extracts were prepared from fresh fecal pellets by vortexing in PBS containing 0.02% NaN₃ and 1 mM PMSF (10 μ L/mg feces). NP-specific Ab from mice immunized with NP₁₆-CGG was measured using plate-bound NP₃₃-BSA or NP₃-BSA. Affinity profiling ELISA was performed as described in ref. 2. Anti-NP antibodies in serum samples (1:100 dilution) were allowed to bind to NP₃₃-BSA ELISA plates. After regular washing, bound antibodies were treated for 10 min at RT with NaSCN solutions (Sigma-Aldrich) each column receiving stepwise increments: 0.05, 0.1, 0.25, 0.5, 1, 2, 2.5, 3, 3.5, 4, and 5 M. Remaining antibodies were detected by AP-conjugated secondary antibodies.

1. Schwenk F, Baron U, Rajewsky K (1995) A cre-transgenic mouse strain for the ubiquitous deletion of loxP-flanked gene segments including deletion in germ cells. *Nucleic Acids Res* 23:5080–5081.

2. Luxton RW, Thompson EJ (1990) Affinity distributions of antigen-specific IgG in patients with multiple sclerosis and in patients with viral encephalitis. *J Immunol Methods* 131:277–282.

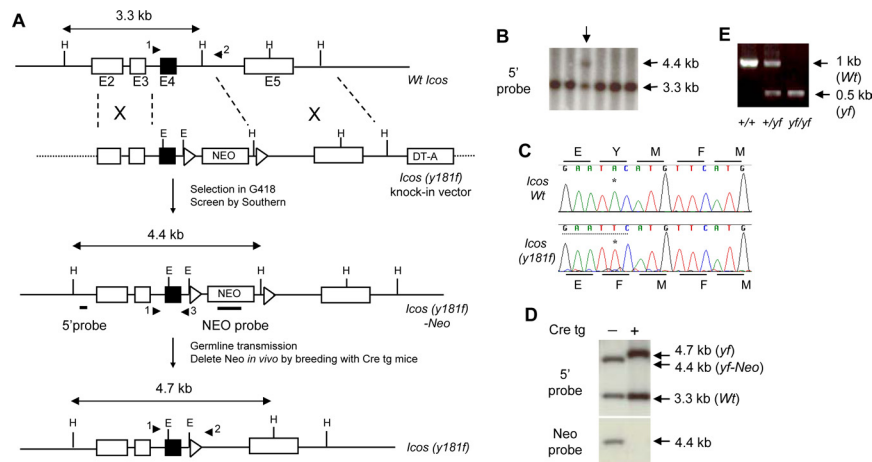


Fig. S1. Generation of ICOS-YF mice. (A) The targeting vector was constructed with Neo cassette flanked by two loxP elements for positive selection and DT-A for negative selection. The exon 4 containing Tyr-181 residue is represented with a filled box, the Southern blot probes are denoted with thick underlines, and PCR primers are shown as arrow heads. (B) Southern blot screening of ES clones using *Hind*III-digested ES genomic DNA. (C) Genomic DNA from ES cells positive for *Icos* (*y181f*)-*Neo* locus was PCR-amplified using primers 1 and 3 as depicted in A, and the nucleotide sequences of the PCR products were determined. Asterisks indicate the A-to-T mutation that results in Tyr-to-Phe mutation with an *Eco*RI site. (D) Genomic DNAs from mice possessing one copy of *Icos* (*y181f*)-*Neo* locus without or with Cre transgene were analyzed by Southern blot after *Hind*III digestion. (E) The genotype of F2 progeny of heterozygous interbreeding was determined by PCR using primers 1 and 2 as shown in A.

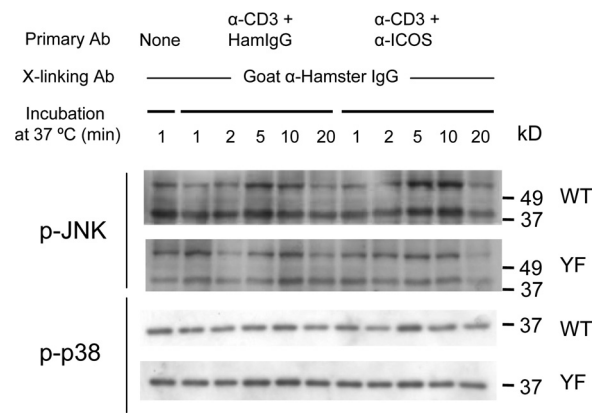


Fig. S3. ICOS does not activate JNK and p38. CD4⁺ T blasts were stimulated with indicated antibodies up to 20 min, and the amounts of phospho-JNK and phospho-p38 were assessed by immunoblotting.

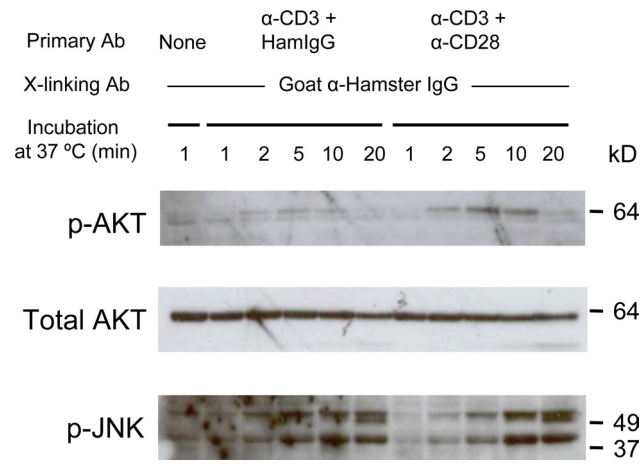


Fig. S4. Moderate activation of AKT by CD28. CD4⁺ T blasts were stimulated with indicated antibodies up to 20 min, and the amounts of phospho-AKT, total AKT, and phospho-JNK were assessed by immunoblotting.

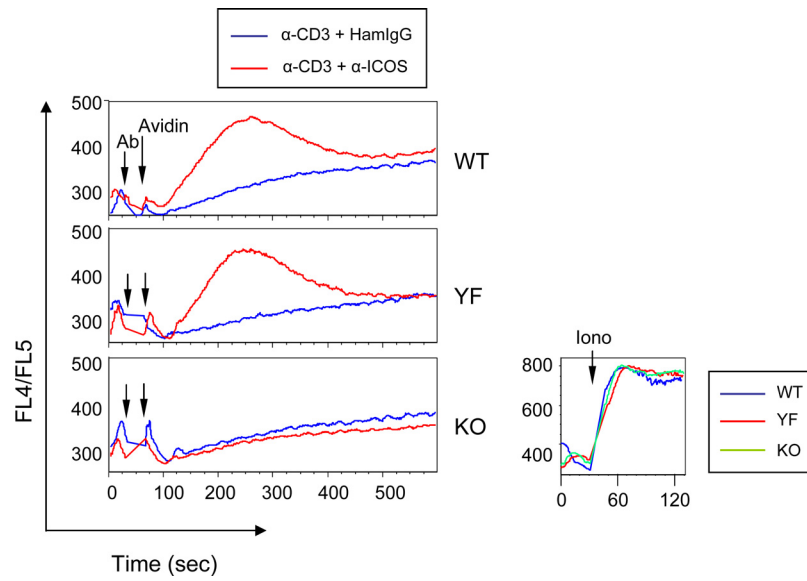


Fig. S5. Intact calcium mobilization by ICOS-YF. Indo-1 loaded CD4⁺ T blasts were stimulated with suboptimal anti-CD3 without or with anti-ICOS, and the intracellular calcium flux was monitored by flow cytometry. A representative of four independent experiments is shown.

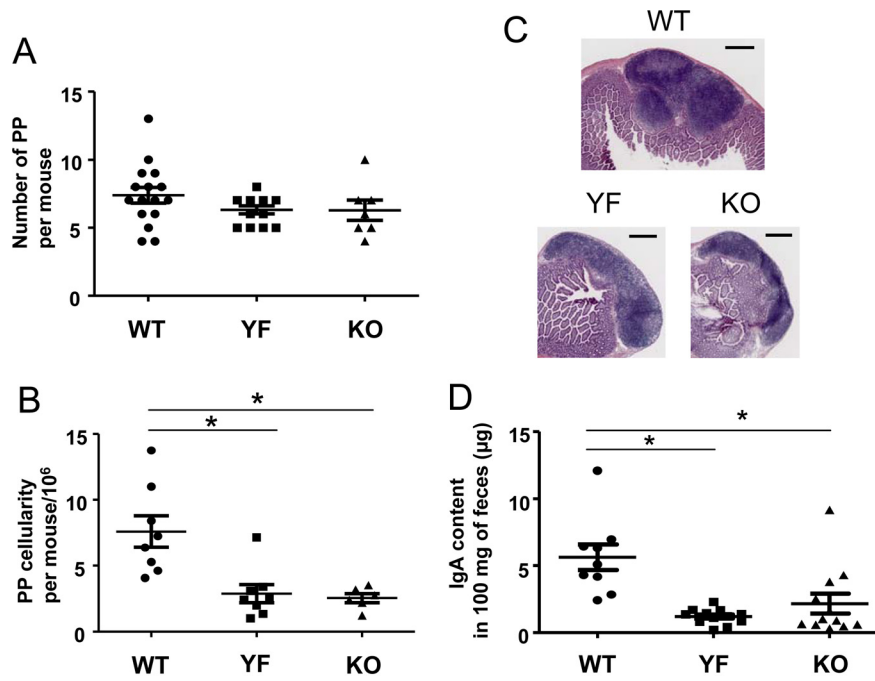


Fig. S6. Normal number of PPs with decreased GC reaction in ICOS-YF and KO mice. (A) Each data point represents the number of PPs per mouse ($n = 10$ WT, 10 YF, and 6 KO). (B) Each data point represents the total number of PP cells collected from a single mouse ($n = 8$ WT, 8 YF, and 6 KO). *, $P < 0.01$. (C) Representative sections of PPs stained with H&E are shown. (Scale bars, $250 \mu\text{m}$.) (D) Decreased mucosal IgA secretion in the gut. IgA contents in fresh fecal pellets were measured by ELISA. Each data point represents the fecal IgA content of an individual mouse ($n = 9$ WT, 12 YF, and 11 KO). *, $P < 0.01$.

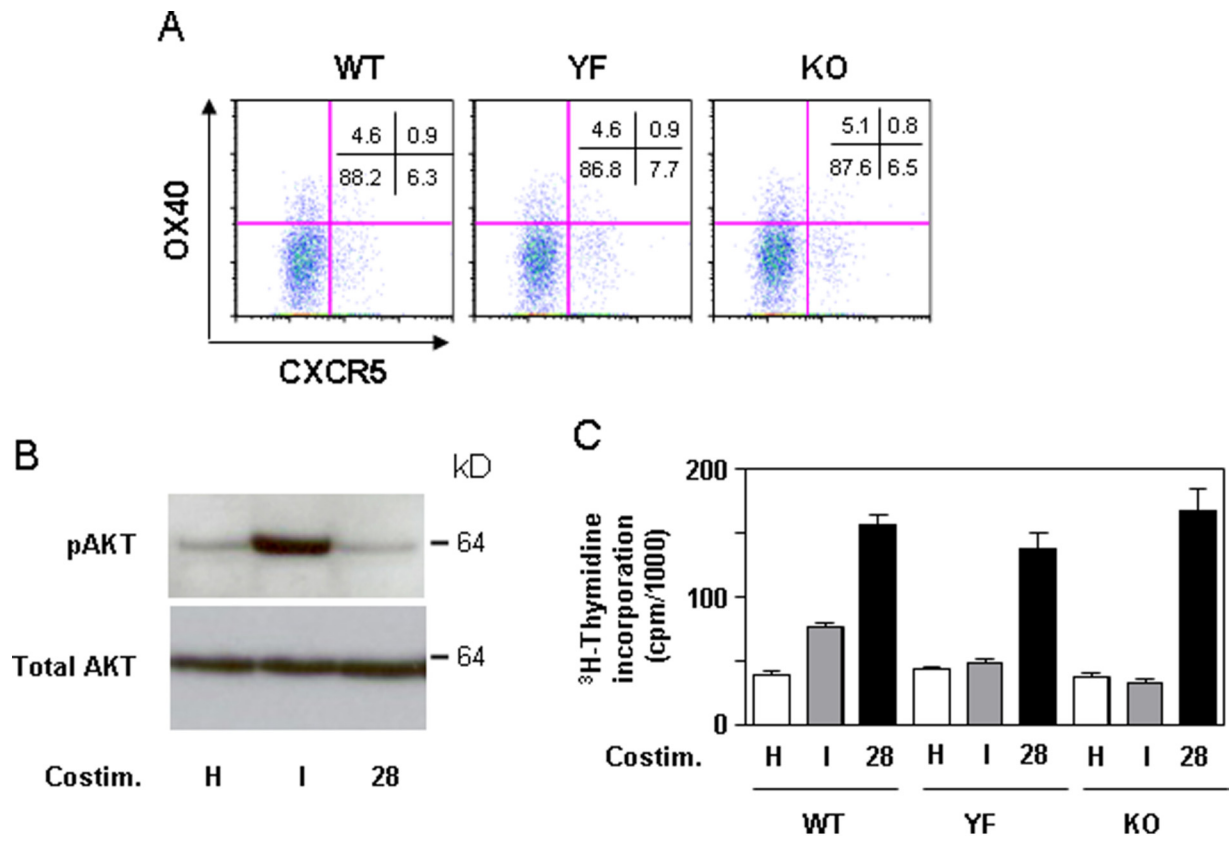


Fig. S7. Differential costimulatory impacts of CD28 and ICOS. (A) Unaltered induction of OX40 and CXCR5 in ICOS-YF and ICOS-KO CD4⁺ T cells. Total lymph node cells were stimulated with soluble anti-CD3 (1 μg/mL) for 2 days, and the levels of OX40 and CXCR5 were analyzed by FACS. A representative of two independent experiments is shown. (B) Differential activation of PI3K pathway by ICOS and CD28. Cell lysates were prepared from CD4⁺ T cells restimulated with anti-CD3 plus hamster IgG (H), anti-ICOS (I), or anti-CD28 (28) followed by goat anti-hamster IgG for 5 min and analyzed by immunoblotting. A representative of two independent experiments is shown. (C) CD28 plays a major role in secondary expansion of CD4⁺ T cells. Cells were restimulated as in B in 96-well plates for 24 h. ³H-thymidine was pulsed for the last 8 h of incubation. A representative of three independent experiments is shown.